Journal of Functional Foods 94 (2022) 105116

Contents lists available at ScienceDirect

Journal of Functional Foods

journal homepage: www.elsevier.com/locate/jff

Apigenin inhibits migration and induces apoptosis of human endometrial carcinoma Ishikawa cells via PI3K-AKT-GSK-3β pathway and endoplasmic reticulum stress

Yan-Cui Liang [a], Qian Zhong [a,b], Run-Hui Ma [a,b], Zhi-Jing Ni [a,b], Kiran Thakur [a,b], Mohammad Rizwan Khan [c], Rosa Busquets [d], Jian-Guo Zhang [a,b], Zhao-Jun Wei [a,b,*]

[a] School of Food and Biological Engineering, Hefei University of Technology, Hefei 230009, China
[b] School of Biological Science and Engineering, Ningxia Key Laboratory for the Development and Application of Microbial Resources in Extreme Environments, North Minzu University, Yinchuan 750021, China
[c] Department of Chemistry, College of Science, King Saud University, Riyadh 11451, Saudi Arabia
[d] School of Life Sciences, Pharmacy and Chemistry, Kingston University London, Kingston Upon Thames, KT1 2EE Surrey, England, United Kingdom

ARTICLE INFO

Keywords:
Apigenin
Apoptosis
ER stress
Mitochondrial pathway
Migration

ABSTRACT

Several experimental and biological studies have emphasized the tumor suppression efficacy and low toxicity of Apigenin (API); however, its exact underlying mechanism on human endometrial carcinoma Ishikawa cell line (EC) is still unknown. We found that API could inhibit the proliferation of Ishikawa cells at IC_{50} of 45.55 μM, arrest the cell cycle at G2/M phase, induce apoptosis by inhibiting Bcl-xl and increasing Bax, Bak and Caspases. Further, API could induce apoptosis by activating the endoplasmic reticulum (ER) stress pathway by increasing the Ca^{2+}, ATF4, and CHOP. It could impede cell migration and invasion through PI3K-AKT-GSK-3β signaling pathway, preventing wound healing, restraining cells migration from the upper chamber to the lower chamber. This study demonstrated that API can be used as a promising dietary supplement and an adjuvant chemotherapeutic agent for cancer treatment.

1. Introduction

Cancer is considered the most alarming life-threatening disease due to the high death and morbidity rate worldwide. Among the various cancer types, endometrial carcinoma (EC), a gynecological malignant tumor, has high incidences which have increased from 56% since 1990 to 21% in the recent years in the developed countries (Prabhakar et al., 2022). The incessant advances in the treatment of EC involve both chemotherapy and radiotherapy which are widely used in anticancer therapy targeting mainly cell cycle arrest and apoptosis induction (Wu, Yang, & Wang, 2019). However, clinical studies reveal that subsequent apoptotic escape leads to adverse effects of chemotherapy (Soto-Gamez et al., 2022). In recent years, studies have focused on the development of new targeted therapies with minimal effects on adjacent normal cells. In this regard, increasing importance is given to plant-derived natural compounds which are constantly proving to be suitable anti-cancer agents for different kinds of targeted therapies in cancer prevention and treatment (Abedul, Daniel, & Arm, 2021).

Natural compounds can induce programmed cell death including apoptosis, necrosis, and pyrosis, thus achieving anticancer effects (Stoner, 2020; Marunaka, Niisato, Zou, Xiao, & Nakahari, 2020). Each type of programmed cell death has its unique characteristics and activation pathways (Abhijit et al., 2022). Cell death caused by apoptosis hinders the occurrence and development of cancer, and many natural

Abbreviations: API, apigenin; DMEM, Dulbecco's modification of Eagle's medium Dulbecco; PS, Penicillin and streptomycin; BCA, bicinchoninic acid; FBS, fatal bovine serum; MTT, 3-(4,5)-dimethylthiahiazo (-z-y1)-3,5-di-phenytetrazoliumromide; PBS, phosphate buffer saline; DMSO, dimethyl sulfoxide; PI, propidium iodide; AV, Annexin V; ROS, reactive oxygen species; JC-1, 5,5′,6,6′-Tetrachloro-1,1′,3,3′-tetraethyl-imidacarbocya nine; PMSF, phenylmethylsulfonyl fluoride; PVDF, polyvinylidene fluoride.

* Corresponding author at: School of Food and Biological Engineering, Hefei University of Technology, Hefei 230009, China.
E-mail addresses: liang18855107789@163.com (Y.-C. Liang), zhong_qian_s@163.com (Q. Zhong), 1120355093@qq.com (R.-H. Ma), lovebear@vip.163.com (Z.-J. Ni), kumarikiran@hfut.edu.cn (K. Thakur), mrkhan@KSU.EDU.SA (M.R. Khan), r.busquets@kingston.ac.uk (R. Busquets), zhangjianguo@hfut.edu.cn (J.-G. Zhang), zjwei@hfut.edu.cn (Z.-J. Wei).

https://doi.org/10.1016/j.jff.2022.105116
Received 8 April 2022; Received in revised form 14 May 2022; Accepted 15 May 2022
Available online 31 May 2022

compounds are reported to induce cell apoptosis. Mitochondria are organelles of eukaryotic cells, involved in intracellular calcium homeostasis regulation, an important source of intracellular ROS, as well as involved in intracellular signal transduction, which is closely related to cell apoptosis (Wang et al., 2022). The members of the Bcl-2 family have distinct effects on apoptosis. Previous studies have suggested that fennel seed extract induced apoptosis of lung cancer cells by down-regulating Bcl-2 (Ke, Zhao, & Lu, 2021). Moreover, ROS is involved in mitochondria-dependent apoptosis (Li et al., 2021). Chimaphilin induced apoptosis of human breast cancer MCF-7 cells through the ROS-mediated mitochondrial pathway (Ma et al., 2014). Another study showed that allicin sensitized the hepatocellular carcinoma cells to the antitumor activity of 5-fluorouracil through the ROS-mediated mitochondrial pathway (Zou et al., 2016). Many researchers have shown that the endoplasmic reticulum (ER) is concerned with the genesis and development of cancer, and it can also be used as a target for cancer treatment. When the ER is stressed, PERK is activated and apoptosis is triggered to eliminate the ER stress cells. It has been suggested that the PERK/eIF2α/CHOP pathway is involved in fumonisin B1-induced cytotoxicity (Yu, Jia, Yang, Liu, & Wu, 2020). Tumor cell migration is an adverse event and one of the important causes of death in tumor patients (Sim et al., 2021). Recent evidence suggest that epithelial-mesenchymal transformation (EMT) plays a key role in tumor metastasis (Kaur, Mukhlis, Natesh, Penta, & Meeran, 2022). The PI3K/AKT/GSK-3β signaling pathway has been reported to affect the expression of epithelial-mesenchymal transformation-related proteins, including MMP2, MMP9, and E-cadherin (Chen et al., 2021). Colorectal cancer cells related studies have shown that PI3K/AKT/GSK-3β signaling pathway is involved in the P2X7 receptor-induced proliferation (Zhang et al., 2021). Previous studies revealed that isohapontigenin (ISO) inhibited EMT in bladder cancer cells; Bashuol, the main component of *Cornus officinalis* root bark, could inhibit the EMT *in vitro* and metastasis of cancer cells *in vivo* (Lee et al., 2021). Therefore, the exploration of novel natural compounds with efficient anticancer activity is the most prominent research area for cancer-related future studies.

So far, many plant bioactive compounds have been shown to exert prominent anti-cancerous effects with low intrinsic toxicity (Abu-Izneid et al., 2020). Among them, polyphenols are the most abundant and flavonoids constitute 60% of all natural polyphenols. Among the flavonoids, 4′,5,7-trihydroxyflavone, known as apigenin (API) exists in edible plant foods. A Japanese study showing the effects of flavonoids on the blood system was also carried out in a seven-day study of 18 healthy men and women, where researchers examined the effects of daily dietary supplements (which provide apigenin in parsley) on platelet aggregation and other hemostatic variables. The authors of this study did not observe significant changes in platelet count, factor VII, plasminogen, PAI-1 activity or fibrinogen concentration induced by collagen or ADP (Nielsen, Young, Daneshvar, Lauridsen, & Knuthsen, 1999). The study also found that total flavonoid intake was inversely associated with plasma total cholesterol and low-density lipoprotein concentrations in women after adjusting for age, body mass index, and total energy intake. These properties classify Apigenin as A beneficial compound with dietary effects that promote health and prevent disease (Maduni, Maduni, Gajski, Popi, & Vrhovac, 2018). Studies have shown that subjects on apigenin-rich diets can systematically absorb apigenin. The results showed that there was no change in the activities of catalase and glutathione peroxidase (Janssen et al., 1998). In previous studies, no significant differences in apigenin absorption or transport were observed between mixed vegetables and snacks using the CaCo-2 Transwell model. Simulated *in vitro* digestion demonstrated a large release of apigenin (Morala et al., 2018). In another study, *in vitro* gastrointestinal digestion model was used to study the bioaccessibility of apigenin, and the results showed that intestinal apigenin content was higher than gastric apigenin content. The bioavailability of apigenin was 20.26 ± 3.06% and 79.74 ± 3.06% after 1 h of gastric juice treatment, while the bioavailability of apigenin was 41.53 ± 13.99% and 58.47 ± 13.99% after 2 h of pancreatic enzyme treatment, respectively. Thus, the bioaccessibility of apigenin suggests that apigenin can be absorbed in the upper intestine, leading to health-related outcomes (Marina, Amin, Loh, Fadhilah, & Kartinee, 2019). Therefore, apigenin may be used as a potential dietary supplement.

API has been investigated in many studies (*in vitro* and *in vivo*) for its anti-cancer effects (Madunic, Maduni, Gajski, Popi, & Garaj-Vrhovac, 2018) associated with antioxidant effects. However, in recent years, studies have reported its effect on cell cycle arrest, counteracting oxidative stress, apoptosis induction, and immunestimulating effects (Dou, Zhou, Ren, & Xu, 2020). API could enhance 5-fluorouracil-induced apoptosis of colorectal cancer cells by regulating thymine synthase (Yang et al., 2021), inhibit hepatocellular carcinoma cell proliferation by up-regulating cleaved caspases-3/8 and down-regulating p-STAT3/p-JAK1/p-JNK2 (Omar et al., 2020). However, the cellular mechanisms underlying the action of API in the induction of cell cycle arrest and apoptosis have not been elucidated on EC Ishikawa cells. Because different phytochemicals have different mechanisms of action on different cancer cells, this study was conducted to evaluate the inhibitory effects of API on the cell viability using EC Ishikawa cells, explore its underlying mechanism for cell cycle modulation, cell apoptosis induction, as well as cell migration and invasion inhibition.

2. Materials and methods

2.1. Chemicals

Apigenin (Muenster, Chengdu, China); DMEM media and serum (Hyclone, Logan, UT); PS (Hyclone, Logan, UT); Trypsin (Hyclone, Logan, UT); PBS (Servicebio, Wuhan, China); MTT (Sigma, St. Louis, MO); primary and secondary antibodies (CST, Danvers, MA; Abcam, Shanghai, China); RT-qPCR kit (Novoprotein, Beijing, China); BCA assay kit (Servicebio, Wuhan, China). SDS-PAGE Gel Preparation Kit (Servicebio, Wuhan, China); Cell Cycle and Apoptosis Analysis Kit (beyotime, Shanghai, China); Annexin V-FITC/PI Double staining Apoptosis Detection Kit (BestBio, Shanghai, China); Reactive Oxygen Species Assay Kit (beyotime, Shanghai, China); Mitochondrial membrane potential assay kit with JC-1 (beyotime, Shanghai, China); Fluo-3 AM (beyotime, Shanghai, China); GSK2656157 and LY294002 (Med Chem Express, Monmouth Junction, NJ).

2.2. Cell culture and treatment

The human endometrial cancer cells (Ishikawa) were incubated in a DMEM medium supplemented with 10% FBS and 1% PS at 37 °C (Zhang et al., 2020). Then, the cells were allowed to grow to more than 80% confluence followed by subculturing with 0.25% trypsin-EDTA. Briefly, cells were seeded in a plate, incubated for 24 h, then treated with API for 48 h. The treated and untreated cells were processed for further experiments.

2.3. Cell viability and cell morphology assay

MTT assay was used to detect the cytotoxicity of API on human endometrial cancer cells. As per previously described methods (Ma et al., 2020), Ishikawa cells (8×10^4 cells/well) were allowed to incubate for 12 h and adhered to the six-well plate walls. The original medium was replaced and Ishikawa cells were co-incubated with various concentration gradients (0, 20, 40, 60, 80, 100, 120, 140, and 160 μM) of API, using 5-FU as the positive control. After the treatment with API for 48 h, the epipelagic medium was discarded and the cells were washed with 150 μL of PBS. Then, 20 μL of 5 mg/ml MTT reagent and 100 μL freshly prepared medium was added, and the cells were incubated for 4 h. Then, 150 μL of dimethyl sulfoxide (DMSO) was added to each well to dissolve formazan (A water-insoluble blue-purple crystal). After 10 mins, the absorbance was detected at 490 nm and 630 nm using

a microplate reader (AMRESCO, Solon, OH).

Based on the MTT results, Ishikawa cells were treated with 0, 30, 50, and 70 μM of API for 48 h, and morphological changes of the Ishikawa cells were scanned using an inverted light microscope (TS100, Nikon, Japan).

2.4. Cell cycle analysis

According to the specification of the cell cycle detection kit and previous experimental results (Yin et al., 2021), Ishikawa cells at the logarithmic growth stage were evenly seeded in a six-well plate at a density of 1×10^5 cells/well and incubated with the fresh medium containing different concentrations of API (0, 30, 50, and 70 μM). Finally, the cells were harvested, fixed with 75% ethanol for 2 h, washed, and stained with propyl iodide (PI) for 30 min at 37 ℃, and red fluorescence was detected by flow cytometry (Beckman Coulter, USA) at the excitation wavelength of 488 nm.

2.5. Detection of apoptosis by Annexin-PI double-staining

According to the instructions of the apoptosis kit and previous experimental results (Liu et al., 2022), Ishikawa cells were treated with different concentrations of API (0, 30, 50, and 70 μM) for 48 h, followed by trypsin digestion. The harvested cells were resuspended in the 1 × Annexin V binding solution and co-incubated with 5 μL Annexin V-FITC staining solution at 4 ℃ for 15 min, followed by co-incubation with 5–10 μL PI for 5 min for flow cytometry analysis (Beckman Coulter, USA).

2.6. Reactive Oxygen Species (ROS) detection

According to the instructions of reactive oxygen species detection kits and previous experimental results (Qin et al., 2021), Ishikawa cells were treated with API (0, 30, 50, and 70 μM) for 48 h followed by trypsin digestion. The final concentration of DCFH-DA was set as 10 μM/L by diluting DCFH-DA with a medium without serum. The collected cells were resuspended in diluted DCFH-DA, incubated for 20 mins, then washed three times. The fluorescence intensity after API treatment was measured by flow cytometry at 488 nm and 525 nm.

2.7. Effect of API on mitochondrial membrane potential ($\Delta\psi m$)

According to the instructions of the mitochondrial membrane potential detection kit and the previously reported method (Li et al., 2021), Ishikawa cells were treated with API (0, 30, 50, and 70 μM) for 48 h and collected into the EP tubes. Cells were resuspended with 500 μL fresh medium and then added with 500 μL JC-1 staining solution, incubated at 37 ℃ for 20 min. Then, the Ishikawa cells were cleaned and resuspended with JC-1 staining buffer (1×), and the fluorescence intensity was detected by flow cytometry and observed by an inverted fluorescence microscope (CKX31; Olympus, Japan).

2.8. Detection for intracellular Ca^{2+} concentration

According to the instructions of the calcium ion fluorescent probe reagent kit and a previous study (Feng et al., 2021), Ishikawa cells were treated with API (0, 30, 50, and 70 μM) for 48 h, washed with PBS, and loaded with 0.5–5 μM Fluo-3 AM. Ishikawa cells were cultivated for 60 min at 37 ℃, then washed appropriately for fluorescence detection by flow cytometry.

2.9. Cell colony formation assay

According to the previous study (Won & Seo, 2020), Ishikawa cells (1000 cells/well) were inoculated in a six-well plate. After 12 h of adherence, Ishikawa cells were incubated with a medium containing different concentrations of API (0, 30, 50, and 70 μM) for 48 h. Subsequently, the medium was replaced once two days for 10 consecutive days. The treated cells were washed properly with PBS, fixed with methanol for 30 min, then stained with 0.1% crystal violet dye for 10 min. After washing off the crystal violet with PBS, the colony count was carried out using Image J. software (BIO-RAD).

2.10. Wound healing assay

According to the previous study (Kim, Kim, & Kim, 2019), Ishikawa cells were seeded in a six-well plate overnight, then draw a straight line at the bottom of the six-well plate with a 200 μL spear tip and took pictures. After cells were treated with API (0, 30, 50, and 70 μM) for 48 h, observed the healing of wounds and took pictures again. The photograph was taken with an inverted fluorescence microscope (CKX31; Olympus, Japan).

2.11. Cell migration and invasion

Ishikawa cells were treated with API (0, 30, 50, and 70 μM) for 48 h. Cell suspensions of 5×10^4 density were prepared in a fresh medium without serum. The 200 μL cell suspensions were moved into each upper chamber. At the same time, 600 μL complete medium was moved into the lower chamber. After migration or invasion for 24 h, the upper chamber was washed three times with PBS, fixed for 30 min, then the methanol was washed with PBS. The cells were stained with crystal violet solution for 20 min, then observed with a light microscope (CKX31; Olympus, Japan). For the invasion experiment, a similar procedure was followed as for the migration experiment. Matrix glue was added into the upper chamber and allowed to be solidified at 37℃ followed by inoculation of Ishikawa cells (Ma et al., 2020).

2.12. RT-qPCR

Total RNA of Ishikawa cells was extracted with Trizol reagent after treatment with API (0, 30, 50, and 70 μM) for 48 h. For this, 1 mL of Trizol reagent was added to each set of samples followed by cell shedding and transfer to 1.5 mL EP tubes. Then, 200 μL chloroform was added to each tube, vortexed for 30 s and left for 5 min. The obtained suspension was centrifuged at 4 ℃ and 12000 rpm for 15 min to stratify the liquid. The upper water phase was transferred to new EP tubes, and isopropyl alcohol was added in equal volume and allowed to stand for 10 min after oscillating followed by centrifugation at 12,000 rpm at 4 ℃ for 10 min. The white precipitate at the bottom of the EP tubes was collected as total RNA. The supernatant was washed and precipitated with 75% ethanol. After drying, the value of A260/A280 (1.8–2.0) was measured. Total RNA was reverse transcribed using a reverse transcription kit. The details are as follows: 1 μL gDNA clean Reagent, 2 μL 5 × gDNA clean buffer, and appropriate volume of total RNA (total RNA not exceeding 1 μg) were added into the 200 Âμl EP tubes, supplemented with RNase free water to 10 μL, reacted at 42 ℃ for 2 min. Then, 1 μL EVO-M−MLvrtase Enzyme Mix, 1 μL RT-Primer Mix, 4 μL 5 × RTase Reaction Buffer Mix 1 and 4 μL RNase free water were mixed and allowed to react at 37 ℃ for 15 min and then further allowed to react at 85 ℃ for 5 sec, and heat preservation at 4 ℃. After reverse transcription, the relative mRNA expression level was evaluated using Light Cycler 96 system using the 2-ΔΔCt method and β-actin as an internal reference gene (Ma et al., 2020). The details are as follows: 10 μL of SYBR, 1 μL of cDNA, 7 μL of DEPC water, 1 μL of forward and 1 μL of reverse (Table 1) were added to each well.

2.13. Western blot

After the total protein was extracted, the BCA kit was used for protein concentration determination. Briefly, Ishikawa cells were treated with API (0, 30, 50, and 70 μM) for 48 h, then cell samples were lysed with

Table 1
Primers for quantitative real-time PCR.

Gene	Primer	Sequence (5′-3′)
CHK2	Forward	CCAGCCAGTCCTCTCACTCCAG
	Reverse	GTTCTTGGTCCTCAGGTTCTTGGTC
p53	Forward	CTACTGGGACGGAACAGCTTTGAG
	Reverse	CTTGCGGAGCCGTGTGCCATTGTG
p21	Forward	GAACTTCCAGCACCGTGTCCAC
	Reverse	TGTCCAGGATGTTCTGCCATTGTG
Cdc2	Forward	GGAAGTCGGCAAAGAGGTACAGGTC
	Reverse	CGAACGAGGAGCTGCTGAAGAC
Cyclin B	Forward	GCTTTGAGGAAGGAGGTGAAGG
	Reverse	AGAGGAGGGCTCGGACACAATC
Bad	Forward	GCCAACCAGCAGCAGCCATC
	Reverse	CCCCATCCCTTCGTCGTCCTC
Bax	Forward	ACGGCCTCCTCTCCTACTTT
	Reverse	AAACACAGTCCAAGGCAGCT
Bcl-xl	Forward	GCATTGTGGCCTTTTTCTCC
	Reverse	GCTGCTGCATTGTTCCCATA
Cyto-c	Forward	AAAGGGAGGCAAGCAGAAGACTG
	Reverse	ATTGGCGGGTGTGTAAGATCC
Caspase 9	Forward	GACCAGAGATTCGCAAACCAGAGG
	Reverse	AAGAGCACCGACATCACCAAATCC
Caspase 3	Forward	CGATGCAGCAAACCTCAGGG
	Reverse	AGCACACAAACAAAACTGCTCCT
Caspase 12	Forward	CACCAGTCCTCAGACAGCACATTC AGACTCTGGCAGTTACGGTTGTTG
	Reverse	
Bip	Forward	GGTGGGCCAAAGGATGAAGAG
	Reverse	CCACAAGCCAAACGACTTCC
IRE1α	Forward	CCAGCACCAGCAGTTCCAGAAG CCGTCCTGAGCCGTGTCTCC
	Reverse	
TRAF2	Forward	GGCTGCGGCAAGAAGAAGATCC TCCTGCTGTTTCTCACCCTCTACC
	Reverse	
ASK1	Forward	CGAATATTGCGGTGGTGGAGATGAG
	Reverse	TCGCAGTAGAGGATGATGTTGTTGG
JNK	Forward	GCATCCATCATCATCGTCGTCTGTC
	Reverse	GCTGCTGCTTCTAGACTGCTGTC
XBP1	Forward	TTGGGCATTCTGGACAACTTGGAC AAGGGAGGCTGGTAAGGAACTGG
	Reverse	
ATF6	Forward	GCGGAGCCACTGAAGGAAGATAAG TGTTTGAGTCTTGGGTGCTGCTG
	Reverse	
PERK	Forward	CCACGCCGCTCTTGACAGTC CCAGGCAAACAAGGTCCCATCC
	Reverse	
eif2α	Forward	GCCGAGGTGACTGTGGAGGAC GTCGCAACTCTGTCTCATCGTCTG
	Reverse	
ATF4	Forward	ATGGATTTGAAGGAGTTCGACT AGAGATCACAAGTGTCATCCAA
	Reverse	
CHOP	Forward	CCCTCCCGTCTCCTCAAAGT CCATTCCTCTCTCGGACGGT
	Reverse	
PI3K	Forward	CTGCGAAATCTGAAGTGCGG CACCTTGCGCCATTTGAGAC
	Reverse	
AKT	Forward	CCTTCTTGGCCTGGGAGAAC CACACGATACCGGCAAAGAA
	Reverse	
GSK-3β	Forward	AGACGCTCCCTGTGATTTATGT
	Reverse	CCGATGGCAGATTCCAAAGG
Snail1	Forward	CCTCGCTGCCAATGCTCATCTG
	Reverse	AGCCTTTCCCACTGTCCTCATCTG
Slug	Forward	CGAACTGGACACACATACAGTG
	Reverse	CTGAGGATGTCTGGTTGTGGT
β-catenin	Forward	AAAGCGGCTGTTAGTCACTGG
	Reverse	CGAGTCATTGCATACTGTCCAT
MMP2	Forward	CGCCTTTAACTGGAGCAAA
	Reverse	AGGTTATCGGGGATGGC
MMP9	Forward	ACGCAGACATCGTCATCC
	Reverse	CCAGGGACCACAACTCG
Vimentin	Forward	AGTCCACTGAGTACCGGAGAC
	Reverse	CATTTCACGCATCTGGCGTTC
E-cadherin	Forward	AGCAGCCCCTTGTAAGC
	Reverse	ACTCCGTGGCATCTGTTC
N-cadherin	Forward	GACAATGCCCCTCAAGTGTT
	Reverse	CCATTAAGCCGAGTGATGGT
β-actin	Forward	TCTCCCAAGTCCACACAGG
	Reverse	GGCACGAAGGCTCATCA

150–300 μL cell lysis buffer (Beyotime, Shanghai, China) for 30 min. The supernatant was centrifuged and placed into new EP tubes. The BCA kit was used to determine the protein concentration. After determining the protein concentration, the loading buffer was added to each EP tube and heated at 98.3 ℃ for 10 min and then allowed to cool down for 5 min. The extracted protein was stored at −80 ℃ for later use. Then, the SDS-PAGE was used and blotted onto a PVDF membrane. The details are as follows: under the condition of 80 V, the protein bands were pressed to a line so that the proteins with different molecular weights were at the same starting line, and then the markers were separated under the condition of 100 V. Finally, the proteins were separated at 120 V. The protein was transferred to PVDF membrane at 130 V and 250 mA. The 5% skim milk diluted by PBST was used to seal the PVDF membrane for 2 h, and then the membrane was cleaned with PBST three times for 10 min each time. The primary antibody (1:1000 dilutions) was incubated on the membrane and kept overnight at 4 ℃. Then the membrane was cleaned with PBST three times for 10 min each time, and co-incubated with the secondary antibody (1:3000 dilutions) on a shaker at 37 ℃ and 80 rpm for 1 h. Then the membrane was cleaned with PBST three times for 10 min each time again. Finally, exposed by the Molecular Imager system (Thermo Scientific, USA), the quantization of protein was carried out using Image J. software (BIO-RAD) (Ma et al., 2020).

2.14. Statistical analysis

All the obtained data were presented as mean ± standard deviation (SD) ($n \geq 3$) before analysis by IBM SPSS Statistics 20 and Origin 2018 at a significant difference of $p < 0.05$.

3. Results

3.1. Inhibitory effects of API on Ishikawa cell activity and morphology

To evaluate the cell survival and growth, Ishikawa cells were treated with API for 48 h. Ishikawa cells were the most sensitive to API in the concentration range of 20–60 μM with an IC_{50} value of 45.55 μM, lower than that of 5-FU (54.20 μM) in the control group (Fig. 1A). Cell morphology was also changed after API treatment for 48 h (Fig. 1B). In

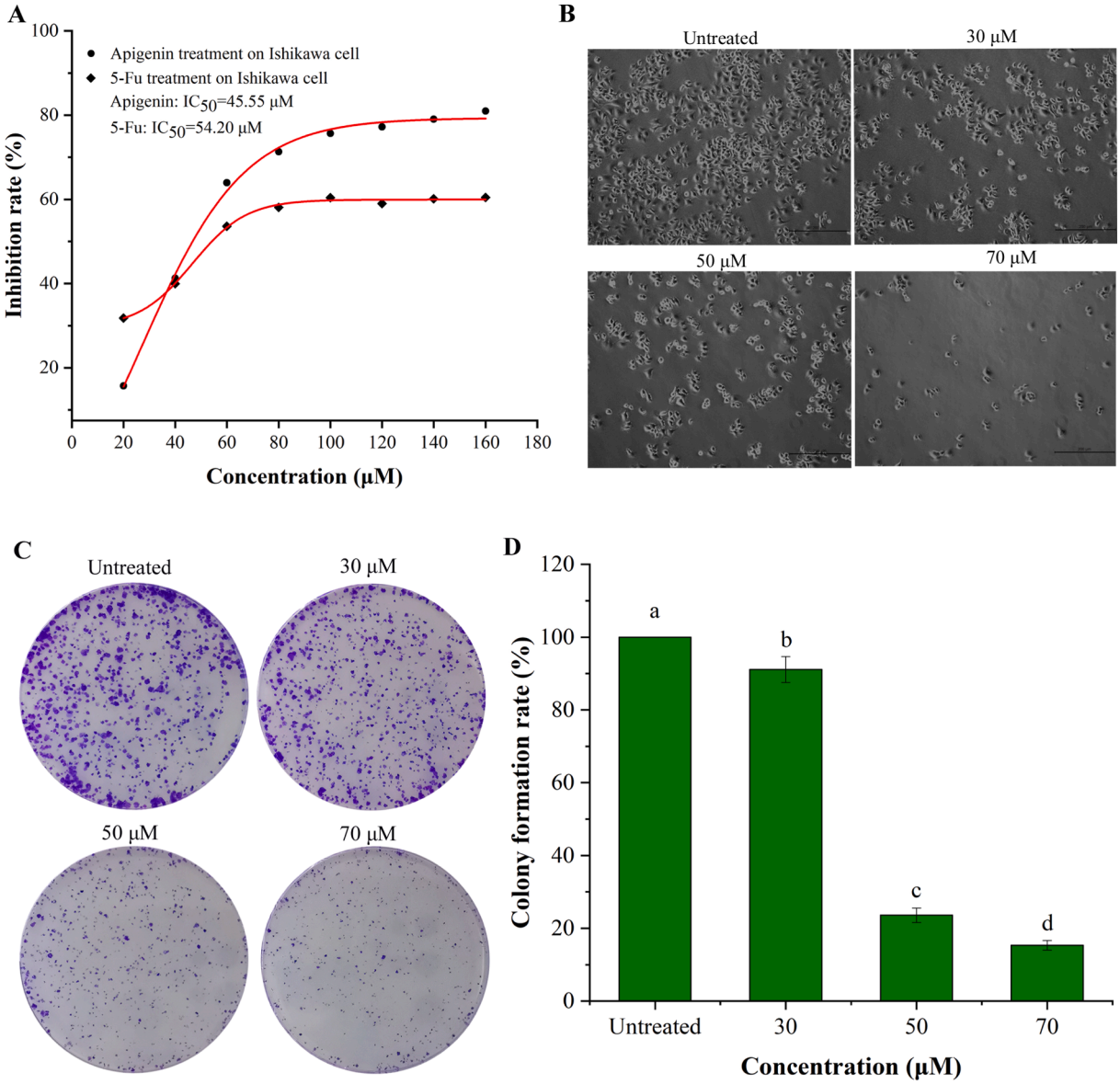

Fig. 1. Inhibitory action and morphological changes of API on Ishikawa cells. (A) Inhibition rate of API and 5-FU on the proliferation of Ishikawa cells. (B) Morphological changes. (C) The colony formation after API treatment. (D) The quantitative analysis of data mentioned in API inhibits colony formation. The data were presented as means ± SD of triplicates experiments.

the control group, the cells appeared as polygonal, grew vigorously, and adhered firmly to the wall. After API treatment, the cell morphology was changed, the cells were shrunken and the antenna disappeared. Compared to the untreated group, the 70 μM treatment group showed the most significant morphological changes which indicated that the changes in cell morphology were dose-dependent.

Cell colony assay is a way to measure cell viability, which avoids the experimental error caused by counting dead cells or non-dividing cells. According to Fig. 1C and D, the colony formation rate of Ishikawa cells decreased significantly with the increase of API concentration, showing a dose-dependent trend.

3.2. Effects of API on cell cycle

After API treatment for 48 h, Ishikawa cells were aggregated at the G2/M phase. PI is a kind of fluorescent dye that can bind to double-stranded DNA to produce fluorescence, and when the content of ds DNA in cells was increased, the fluorescence intensity was also increased. Based on the above principle, according to the experimental results in Fig. 2A and B, the proportion of the G2/M phase cells was 22.36% in the untreated group, 27.09% in the 30 μM treatment group, 31.37% in the 50 μM treatment group, and 39.38% in the 70 μM treatment group. To further explore the molecular mechanism of aggregated cells at the G2/M phase, the mRNA and protein expression levels of key regulatory factors in the G2/M phase were evaluated. As

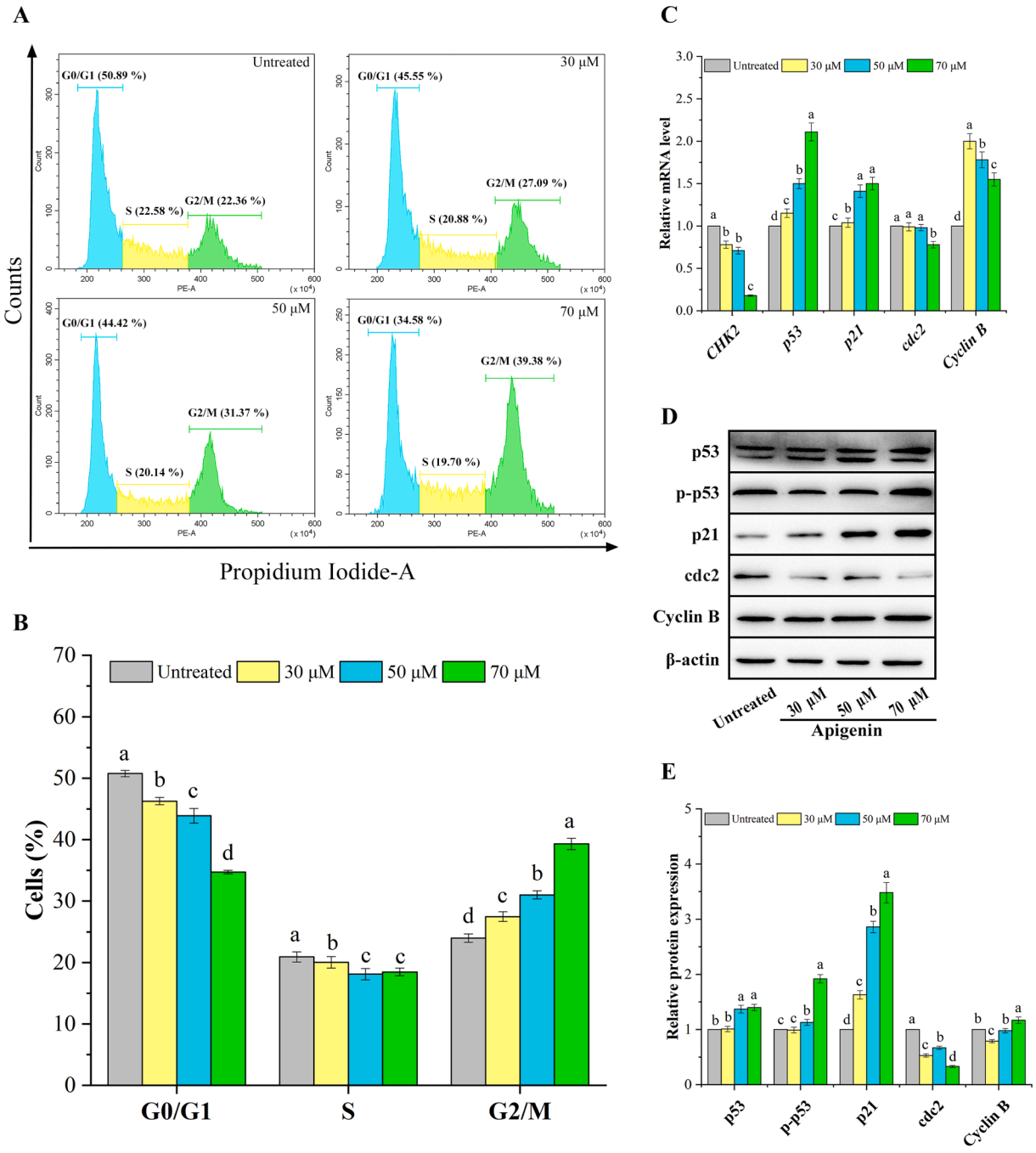

Fig. 2. API arrested Ishikawa cells at G2/M phase and the cycle-related gene and protein. (A) Cell cycle distribution of Ishikawa cells after API treatment. (B) The proportion of cell cycle in different phases. (C) Relative mRNA level. (D) Relative protein bands by Western blotting analyses. (E) The quantitative protein expression of data mentioned in (D). Values were means ± SD of three replicates. Different letters represent significant differences between two groups ($p < 0.05$).

shown in Fig. 2C, mRNA levels of cell cycle-related key genes such as *CHK2* and *cdc2* were down-regulated, while that of *p53* and *p21* were up-regulated. Fig. 2D confirmed the expression levels of cell cycle-related proteins, and Fig. 2E represented the relative expression of related proteins. The amount of translation of cell cycle key proteins was consistent with that of mRNA, with the rising amount of translation of p-p53 and p21, and the decrease in cdc2.

3.3. Effects of API on cell apoptosis

As demonstrated in Fig. 3A and B, the proportion of early apoptotic cells increased gradually with the increase of API concentration. The relative percentage of early apoptosis in 30 μM, 50 μM, and 70 μM groups increased by 14.22%, 22.64%, and 27.79%, respectively. The membranes of normal and early apoptotic cells were intact, and Annexin V-FITC could bind to PS when phosphatidylserine was evaginated on the membranes of early apoptotic cells. Annexin V-FITC could also bind to PS when the membranes of late apoptotic cells and necrotic cells were broken. PI could not bind to the nucleic acid of normal and early apoptosis cells but could bind to the nucleic acid of the middle and late apoptosis cells.

3.4. Effects of API on ROS generation and mitochondrial membrane potential (MMP)

ROS promotes apoptosis mainly via increasing the permeability of the mitochondrial membrane, thereby releasing Ca^{2+} and Cyto-c, leading Caspase-9 to activate Caspase-3 and reducing MMP. The non-fluorescent DCFH probe is oxidized by intracellular ROS into fluorescent DCF, thus the amount of intracellular ROS can be detected. According to the results of Fig. 4A and B, the level of intracellular ROS increased gradually with the increase of API concentration. According to Fig. 4C, with the increase of API concentration, the fluorescence gradually changed from red to green, indicating the decrease in MMP. We also quantified the decrease of MMP, and Fig. 4D and E showed that mitochondrial membrane potential of 30 μM, 50 μM, and 70 μM groups decreased by 2.19%, 11.32%, and 14.91%, respectively.

To further study the underlying molecular mechanism of apoptosis, we determined the key mRNAs and proteins of the mitochondrial signaling pathway. According to the results in Fig. 4F, API increased the relative mRNA expression of pro-apoptotic genes *Bad*, *Bak*, and *Cyto-c*, down regulated the anti-apoptotic genes *Bcl-xl*, and the mRNA level of *Caspase-9* and *Caspase-3* were also decreased. According to Fig. 4G and H, the protein levels of Bad, Bak, Cyto-c, Caspase-9, and Caspase-3 were up-regulated, while the protein levels of Bcl-xl were down-regulated indicating the role of mitochondrial signaling pathway in API induced apoptosis.

3.5. Effects of API on Ca^{2+} and endoplasmic reticulum stress

Calcium homeostasis is involved in maintaining normal structure and function in the cell. Fluo-3/AM can be decomposed by intracellular esterase into Fluo-3, which can bind with intracellular Ca^{2+}, and the fluorescence intensity becomes stronger with the increase of Ca^{2+} concentration. According to the results of Fig. 5A and B, after API treatment for 48 h, the intracellular Ca^{2+} concentration increased in cells in a dose-dependent manner. When the concentration of Ca^{2+} in ER is unbalanced, it can lead to ER stress, and continuous ER stress can lead to cell apoptosis. To verify that ER stress is involved in cell apoptosis, key genes and proteins of ER stress were detected after API treatment. As shown in Fig. 5C, D, and E, the mRNA levels of *IRE1α*, *TRAF2*, *XBP1*, *ATF6*, *eIF2α*, *ATF4*, and *CHOP* were up-regulated, and the mRNA levels of *Caspase-12*, *Bip*, *ASK1*, *JNK*, and *PERK* were down-regulated. The protein levels of Caspase-12, IRE1α, p-JNK, eIF2α, p-eIF2α, ATF4, and CHOP were up-regulated, while the protein levels of JNK1, JNK2, and PERK were down-regulated. After pretreatment with PERK inhibitor GSK2656157 (Fig. 5F and G), the inhibition of API on PERK and the promotion of ATF4 and CHOP were alleviated which indicated that ER stress was involved in apoptosis after API treatment for 48 h.

3.6. Inhibitory effects of API on cell migration and invasion

To explore whether API can reduce the migration and invasion ability of Ishikawa cells, we conducted cell wound healing experiments, and the results are shown in Fig. 6A and B. After 48 h of healing, the number of cells migrating to the gully in the untreated cells was distinctly elevated than that in the API treated cells. Transwell experiment results in Fig. 6C and D also showed that the migration and

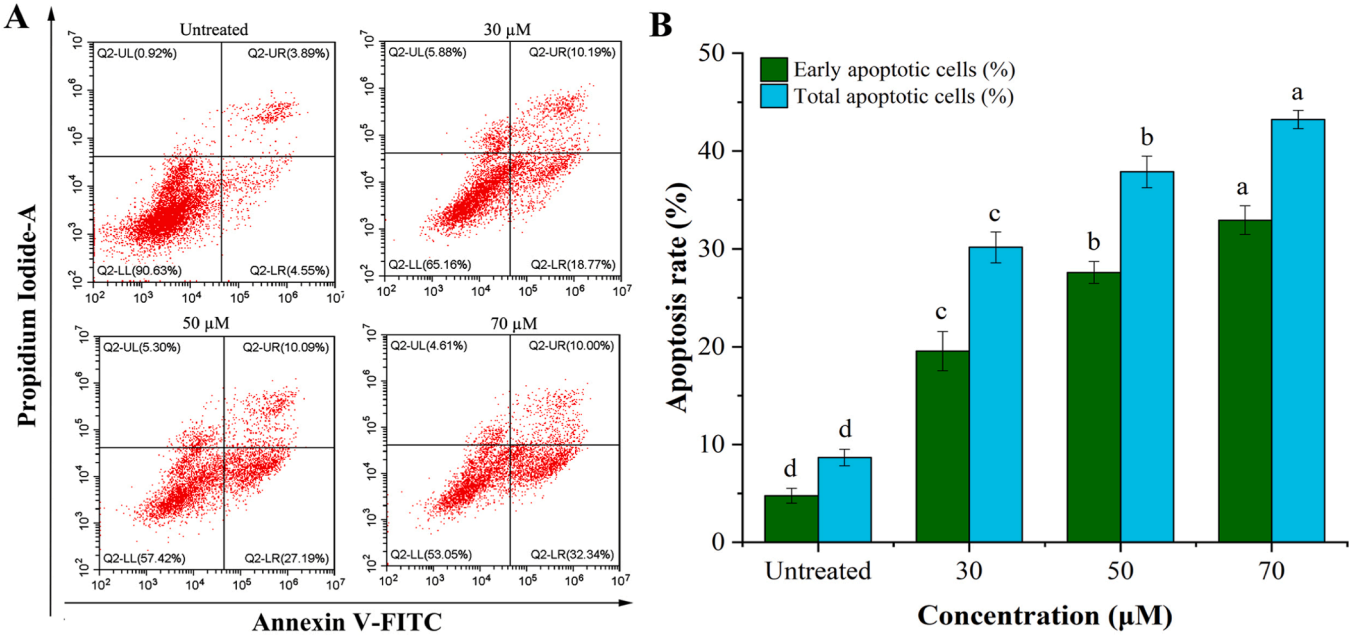

Fig. 3. API promotes Ishikawa cells apoptosis. (A) Cell distribution diagram of double staining with Annexin V/PI by flow cytometry. (B) The quantitative analysis of data mentioned in (A). Values were means ± SD of three replicates. Different letters meant significant differences between two groups ($p < 0.05$).

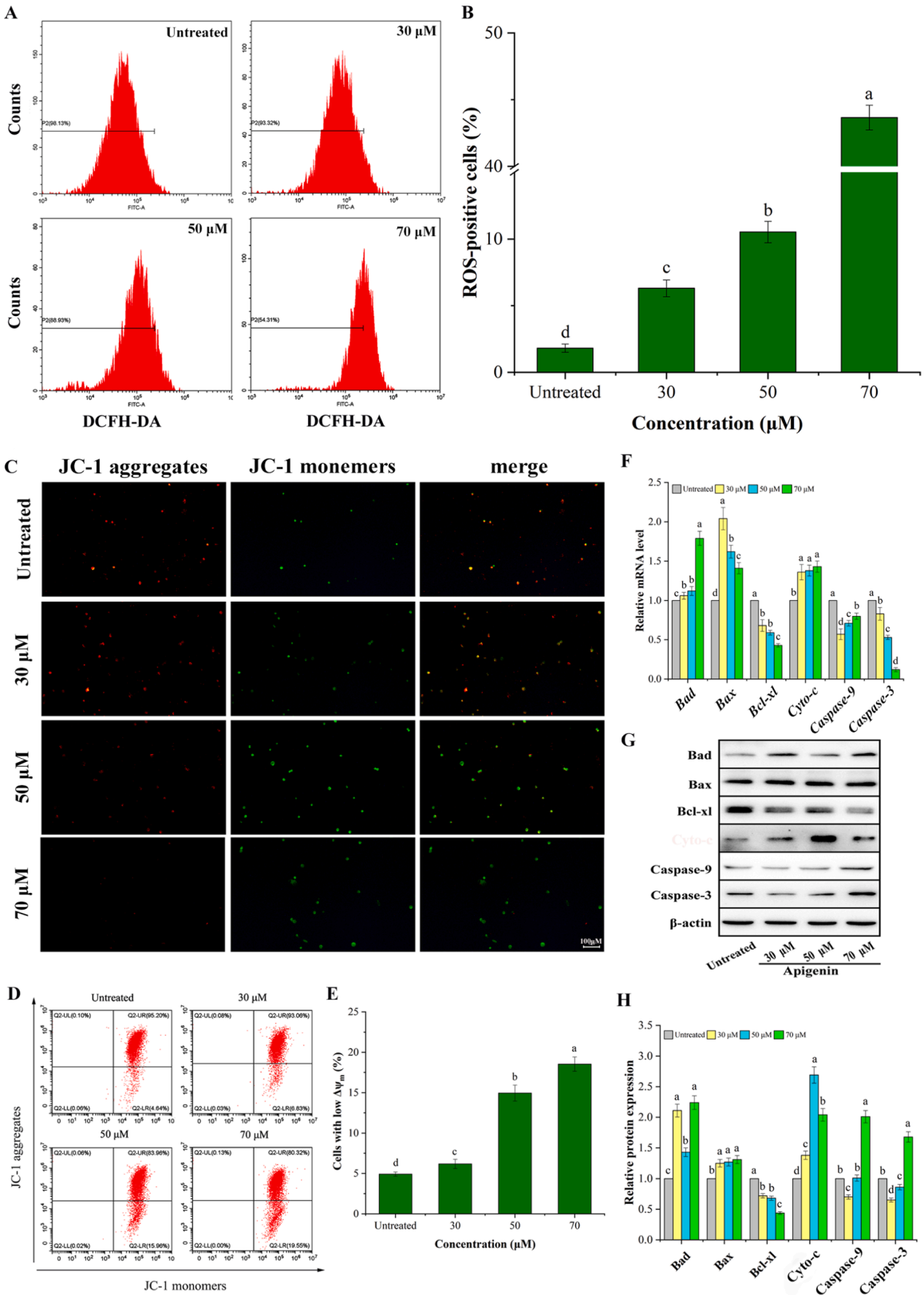

Fig. 4. API increases ROS production, reduces mitochondrial membrane potential in Ishikawa cells and the mitochondrial pathway related gene and protein. (A) The percentage of ROS-positive cells after API treatment. (B) The quantitative analysis of data mentioned in (A). Values were means ± SD of three replicates. Different letters meant significant differences between two groups ($p < 0.05$). (C) Immunofluorescence photographing of JC-1 staining for *Δψm*. (D) Δψm was assessed by flow cytometry. (E) Percentage of cells with Δψm loss. (F) Relative mRNA level. (G) Relative protein bands by Western blotting analyses. (H) The quantitative protein expression of data mentioned in (G). Values were means ± SD of three replicates. Different letters represent significant differences between two groups ($p < 0.05$).

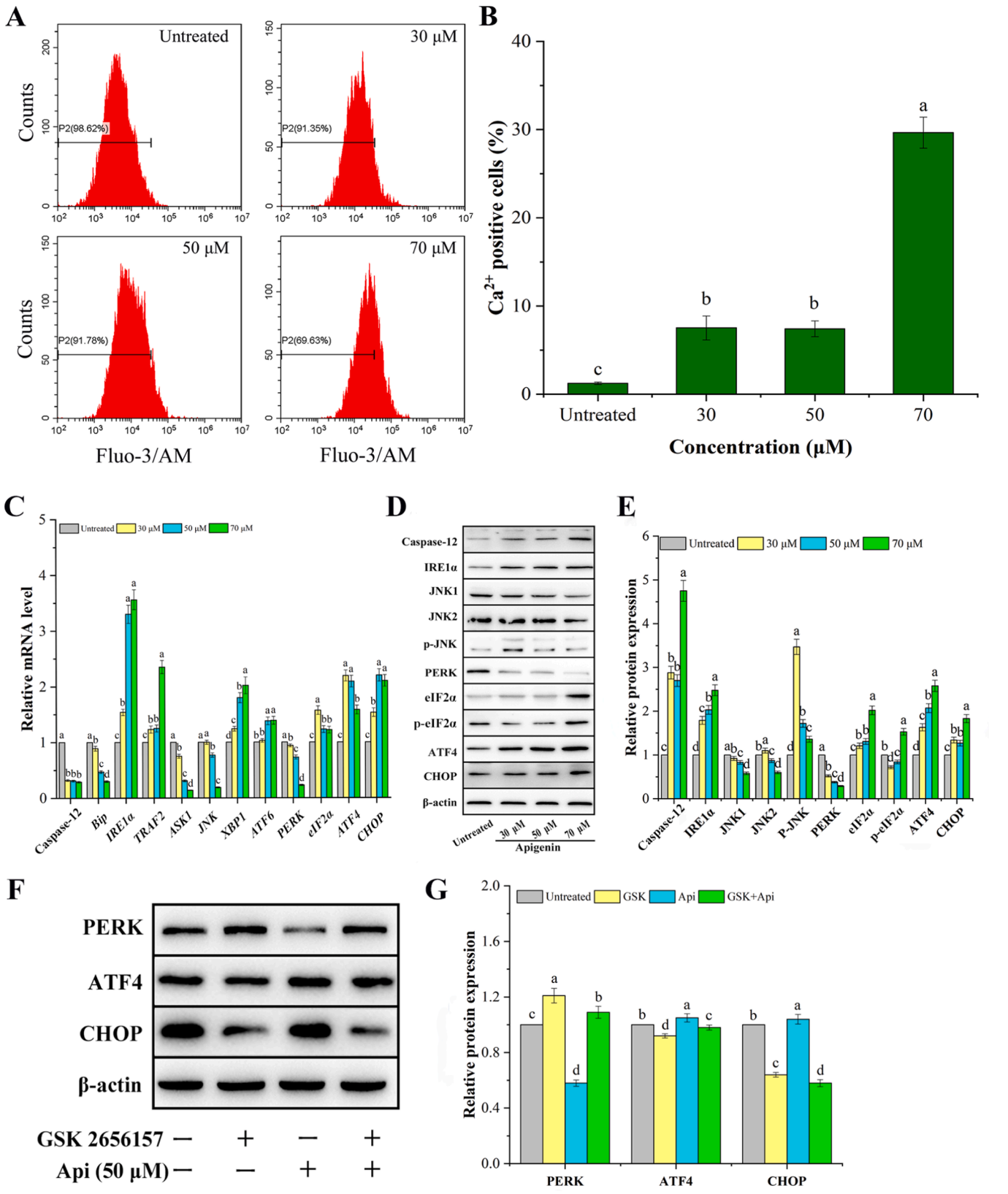

Fig. 5. API increases Ca^{2+} production and the ER stress related gene and protein. (A) The percentage of Ca^{2+}-positive cells after API treatment. (B) The quantitative analysis of data mentioned in (A). Values were means ± SD of three replicates. Different letters meant significant differences between two groups ($p < 0.05$). (C) Relative mRNA level. (D) Relative protein bands by Western blotting analyses. (E) The quantitative analysis of protein expression data mentioned in (D). (F) Effect of PERK inhibitor (GSK2656157) on API-induced apoptosis of Ishikawa cells. (G) The quantitative analysis of protein expression data mentioned in (F).Values were means ± SD of three replicates. Different letters meant significant differences between two groups ($p < 0.05$).

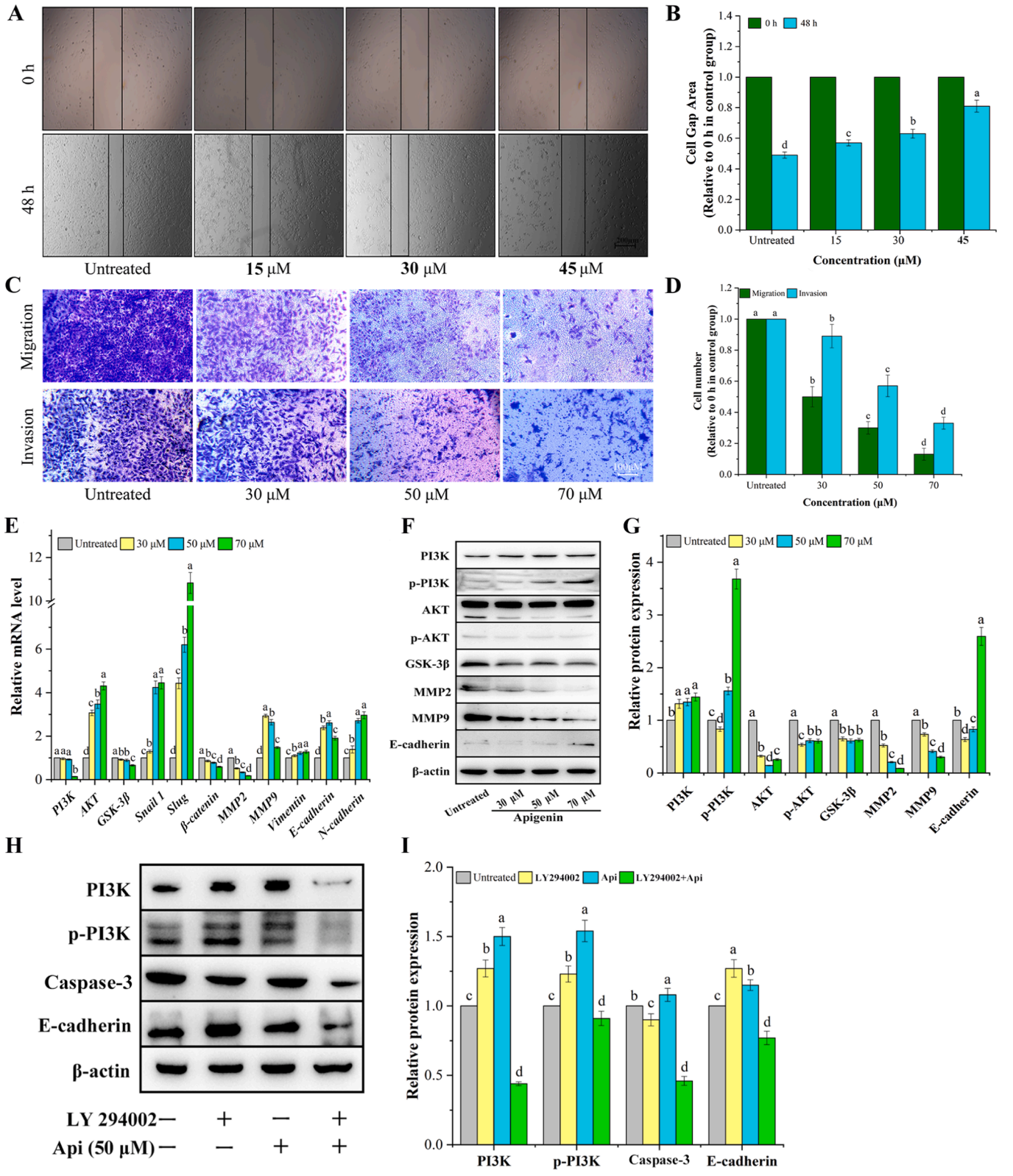

Fig. 6. API inhibits the migration and invasion of Ishikawa cells and the migration and invasion related gene and protein. (A) Wound healing at 0 h and 48 h after scratching the monolayer cells cultured in a 6-well plate. (B) Quantitative form of data shown in (A). (C) API treatment inhibited the migration and invasion ratio of cells from the upper chamber to the lower chamber of the transwell. (D) Quantitative form of data shown in (C) about cell number. Values were means ± SD of three replicates. Different letters meant significant differences between two groups ($p < 0.05$). (E) Relative mRNA level. (F) Relative protein bands by Western blotting analyses. (G) The quantitative analysis of protein expression data mentioned in (F). (H) Effect of PI3K inhibitor (LY294002) on API-induced apoptosis of Ishikawa cells. (I) The quantitative analysis of protein expression data mentioned in (H). Values were means ± SD of three replicates. Different letters meant significant differences between two groups ($p < 0.05$).

invasion rates of Ishikawa cells were comparatively distinctly reduced in the API treated cells. We further investigated the levels of key genes (Fig. 6E) and proteins (Fig. 6F and G) responsible for migration and invasion, we found that the mRNA levels of *Snail1*, *Slug*, *MMP9*, and *E-cadherin* were up-regulated and the mRNA levels of *PI3K*, *GSK-3β*, and *MMP2* were down-regulated in Ishikawa cells after API treatment. Meanwhile, the protein translation levels of p-PI3K and E-cadherin were up-regulated and the protein translation levels of p-AKT, GSK-3β, MMP2, and MMP9 were down-regulated. After pretreatment with PI3K inhibitor LY294002, Ishikawa cells were treated with API for 48 h. As shown in Fig. 6H and Fig. 6I, the promoting effect of API on PI3K, p-PI3K, and E-cadherin was weakened. We speculate that API restrained the migration and invasion of Ishikawa cells. In addition, the promoting effect of API on Caspase-3 was also weakened, indicating the role of the PI3K-AKT signaling pathway in cell apoptosis (Fig. 7).

4. Discussion

Cancer cells are characterized by rapid growth, disordered division, abnormal DNA synthesis, rapid metabolism, and energy production. Chemotherapy and radiotherapy are the most available and commonly-used strategies. Due to their side effects and drug intolerance, the use of chemotherapy agents has been limited (Dehkordi et al., 2021). Uterine cancers, more than 90% of their origin is in endometrium, influence almost 10,000 women in the UK and over 300,000 worldwide each year. Generally, post-menopausal women are more susceptible to this risk (Perera & Hoskin, 2021). Cancer still stands as main causes of mortality worldwide, despite the huge advances in its diagnosis and treatment over the past few decades, killing an estimated 9.6 million people each year. Endometrial cancer is the fourth most common cancer affecting women in the United States, and it is becoming more common in younger women. Early or advanced endometrial cancers with medium–high or high-risk characteristics have a high recurrence rate. In addition, sometimes existing treatments for endometrial cancer do not work well, patients with endometrial cancer still have a very poor prognosis, and sometimes existing drugs do not respond to patients with endometrial cancer, so new treatments are needed (Saripalli, Griffin, Ross, & Roeske, 2022). API is a reliable natural compound known for anti-cancer effects (Yang et al., 2021). API could block the cell cycle, induce apoptosis in hepatocellular carcinoma cells (Yang, Pi, & Wang, 2018) and inhibit cell migration in pancreatic cancer cells (He et al., 2015) through the PI3K-AKT signaling pathway. In our study, API restrained the viability of Ishikawa cells, and the inhibition effect of API on Ishikawa cells was better than that of 5-FU. Our study demonstrated that apigenin has a good inhibitory effect on endometrial carcinoma *in vitro*. However, further *in vivo* and clinical trials are needed to classify apigenin as an anticancer drug (Zhang et al., 2021).

According to previous studies, the cell cycle mechanism is regarded as one of the targets of cancer therapy. The cell cycle is mainly divided into four stages, including G1, S, G2, and M. Cell cycle checkpoints hold

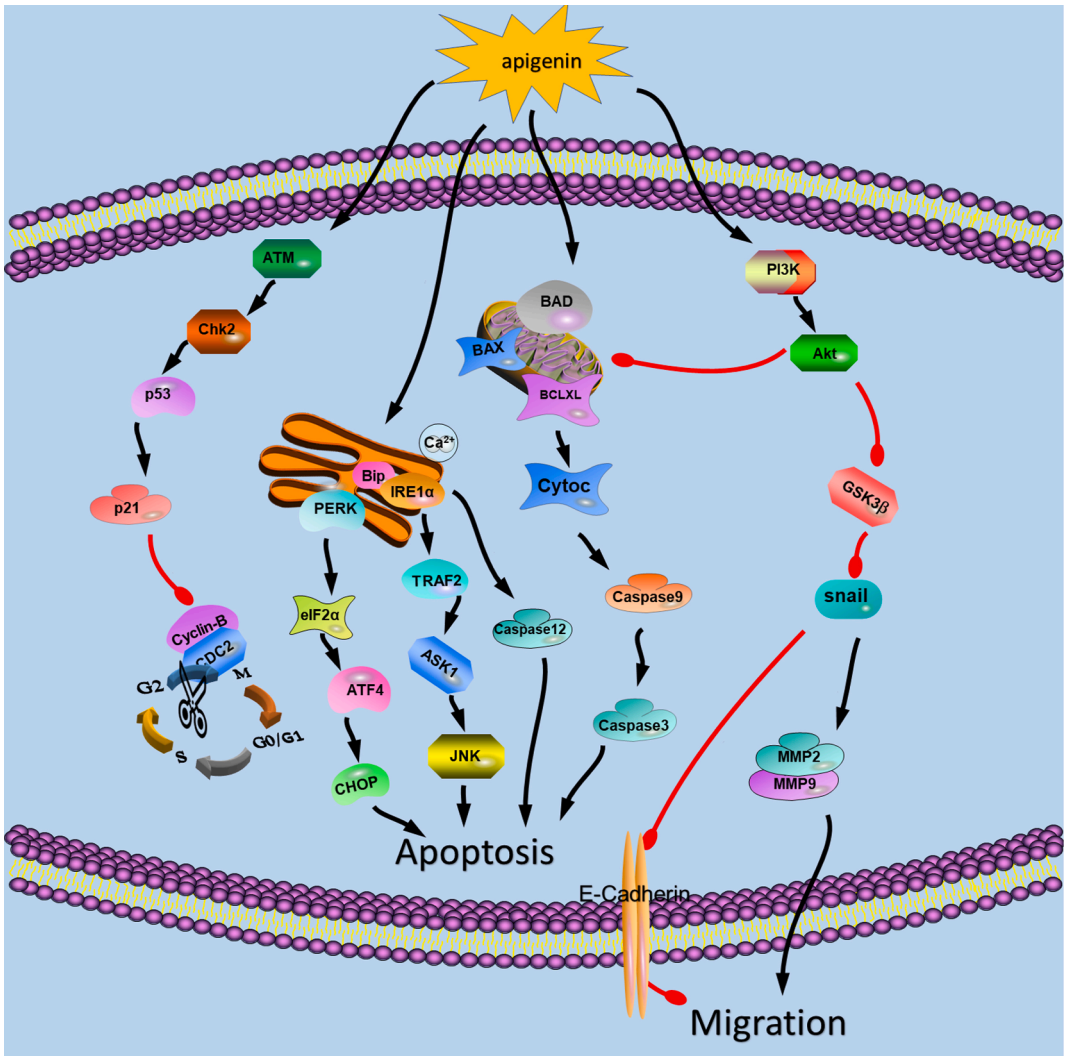

Fig. 7. Possible molecular mechanism behind the anticancer effects API on Ishikawa cells.

an orderly progression from one cell cycle stage to the next. Cell cycle checkpoints included the G1/S checkpoint, G2/M checkpoint, and spindle assembly checkpoint (Liu et al., 2021). One of the most obvious mechanisms is by which API induces p53 tumor suppressor proteins at the translational level and the induces p21 (Lee et al., 2014). Similar to previous studies, we found that API induced p53 and p21 at the translational level, which could block Ishikawa cells in the G2/M phase and further inhibit cell proliferation. Cdc2 is the catalytic subunit of the M stage promoter and is activated when cell transition occurs from G2 to M. Cdc2 also controls the onset of mitosis. It has been reported that the combination of Cdc2 and Cyclin B plays a key role in the transformation from G2 to the M phase (Choi and Kim, 2009). API-treated Ishikawa cells showed increased expression levels of p-p53 and p21. Our results suggested that down-regulation of cdc2 and up-regulation of p-p53 and p21 may be responsible for API-induced Ishikawa cell arrest in the G2/M phase. One of the regulated cell death mechanisms, apoptosis plays a vital role in the removal of cancerous cells (An et al., 2018). According to a previous study, apoptosis is initiated through two principal pathways: extrinsic and intrinsic pathways (Kim et al., 2019). Caspase plays a vital role in the adjustment and control of cell apoptosis (Shrestha & Clark, 2021). The mitochondria are the main regulators of the intrinsic pathway, which activate the intra-cellular caspases. The Bcl-2 family (Manogaran, Beeraka, Huang, & Padma, 2019), including pro-apoptotic and anti-apoptosis proteins, control the discharge of cytochrome *c* and other promote apoptosis proteins, which is contacted with the integrity of the mitochondrial membrane. After the mitochondria release the Cyto-c, the Caspase-9 is activated, resulting in increased activity of Caspases (Vijaya et al., 2018). Over-expression of the Bak and Bad can increase mitochondrial membrane permeability, which is useful for Cyto-c release. ROS is a key factor in tumor genesis and development, and superfluous intracellular aggregation of ROS can lead to apoptosis. When the cells are stimulated by apoptosis signals, ROS aggregation can transform the translation of anti-apoptotic proteins, therefore activating mitochondria-mediated apoptosis. In our study, the expression levels of Bad, Bax, Cyto-c, Caspase-9 and Caspase-3 proteins were up-regulated, while the expression level of Bcl-xl was down-regulated which indicated that the mitochondrial signaling pathway intervened in the API induced apoptosis.

The ER is an intracellular organelle responsible for the folding and complex formation of proteins (Lee, Lee, Kim, & Chae, 2019). The ER stress can be caused by redox alterations, calcium equilibrium, and protein degradation, which leads to the unfolded protein response (UPR). ER stress can improve cell survival by acting against UPR stress, however, persistent ER results in apoptosis through the mutual effect between ER and mitochondria. The stress-activated protein kinase, JNK, plays a significant role to regulate and control apoptosis. It has been proved that ROS plays a key role in the phosphorylation and maintenance of JNK activation (Liu et al., 2021). IRE1α is a transmembrane protein resident in ER and is considered to command UPR signaling pathway. When ER stress is persistent, the activated IRE1α joins TRAF2 and ASK1, leading to the activation of the JNK pathway. It has been proposed that JNK is activated through the formation of the IRE1α-TRAF2-ASK1 complex (Zhang et al., 2016). In addition, under the ER stress, pancreatic ER kinase (PERK) enhances phosphorylation of eIF2α to mediate the UPR. The eIF2α can inhibit Cap-mediated eukaryotic translation initiation. After eIF2α phosphorylation, the ATF4 is presciently up-regulated, which then leads to the activation of CHOP (Jayasooriya et al., 2018). Moreover, Caspase-12 is a key and unique molecule located on the ER membrane that regulates apoptosis through ER stress. Therefore, during ER stress, increased intracellular Ca^{2+} levels activate Calpain, which can generate Caspase-12 through cleavage of procaspase-12. Caspase-12 performs apoptosis by triggering downstream Caspase-9 and Caspase-3 genes (Wu et al., 2020). In our study, the intracellular level of ROS and Ca^{2+} was elevated and the p-JNK, CHOP, and Caspase-12 expression levels were up-regulated. We demonstrated that API could promote apoptosis through the PERK-eIF2α-ATF4-CHOP pathway, IRE1α-TRAF2-ASK1-JNK pathway, and Caspase-12 pathway.

Cancer cell migration is considered to be one of the most important cellular functions in tumor metastasis. Epithelial-mesenchymal transformation (EMT) is characterized by the transformation of epithelial cells into mesenchymal cells through a specific process responsible for tumor metastasis. The primary features of the EMT process include decreased expression level of cell adhesion molecules and replacement of cytokeratin by vimentin in the cytoskeleton to obtain morphological characteristics of mesenchymal cells (Xu et al., 2021). Previous studies have acknowledged the PI3K/AKT/GSK-3β signaling pathway, as a classic signaling pathway in tumorigenesis and its key role in cell growth and metabolism has already been described. Ultimately, it affects the invasion, metastasis, and invasiveness of cancer cells. It has been proved that increased expression levels of MMP2 and MMP9 can accelerate prostate cancer metastasis, and the translation levels of MMP2 and MMP9 are negatively correlated with the prediction of prostate cancer progression (Fan et al., 2021). E-cadherin plays a key role in maintaining epithelial tissue function by forming cell-to-cell adhesion connections. The absence of E-cadherin imparts the capacity of cancer cells to invade and migrate and is therefore considered a hallmark of EMT (Li et al., 2022). Our results showed that API treatment could up-regulate the expression level of E-cadherin and inhibit the translation level of MMP2 and MMP9 in Ishikawa cells, indicating that API could suppress the migration of Ishikawa cells.

5. Conclusion

To summarize, our study reported the significant inhibition of the proliferation of Ishikawa cells after treatment with API (IC_{50} of 45.55 μM). API affected the expression of cycle genes and blocked the cell cycle in the G2/M phase. API interfered with the expression of the Bcl-2 family and induced the apoptosis via mitochondrial signaling pathway. After API treatment, intracellular ROS and Ca^{2+} concentrations were increased, causing intracellular net stress, and inducing apoptosis through Caspase-12, IRE1α-TRAF2-ASK1-JNK, and PERK-eIF2α-ATF4-CHOP pathways. In addition, under the influence of API, the cell adhesion was enhanced through up-regulation of E-cadherin expression level and down-regulation of the MMP2 and MMP9 expression levels, and the ability of migration and invasion was reduced. Our results suggest that API is a natural compound with anti-cancer effects. API can be considered a promising anticancer compound because of its characteristics of safety, low toxicity, and high efficiency. For the future studies, the effects of API on endometrial cancer under *in vivo* conditions are worthy of consideration.

CRediT authorship contribution statement

Yan-Cui Liang: Conceptualization, Methodology, Software, Writing – original draft. **Qian Zhong:** Validation, Investigation. **Run-Hui Ma:** Methodology, Software. **Zhi-Jing Ni:** Methodology, Software. **Kiran Thakur:** Data curation, Investigation. **Mohammad Rizwan Khan:** Methodology, Software. **Rosa Busquets:** Data curation, Writing – review & editing. **Jian-Guo Zhang:** Visualization, Investigation. **Zhao-Jun Wei:** Funding acquisition, Supervision, Writing – review & editing.

Declaration of Competing Interest

The authors declare that they have no known competing financial interests or personal relationships that could have appeared to influence the work reported in this paper.

Acknowledgements

The authors would like to thank the National Natural Science Foundation of Ningxia Province (2021AAC02019), the Major Projects of

Science and Technology in Anhui Province (201903a06020021, 201904a06020008, 202004a06020042, 202004a06020052), the Researchers Supporting Project No. (RSP-2021/138) King Saud University, Riyadh, Saudi Arabia.

References

Abedul, H., Daniel, B., & Arm, R. A. (2021). Perspectives on natura compounds in chemoprevention and treatment of cancer: An update with new promising compounds. *European Journal of Cancer., 149*, 165–183.

Abhijit, C., Li, Y., Zhang, C., Li, Y. M., Scott, A. L., & Ying, H. S. (2022). Programmed cell death in aortic aneurysm and dissection: A potential therapeutic target. *Journal of Molecular and Cellular Cardiology., 163*, 67–80.

Abu-Izneid, T., Rauf, A., Shariati, M. A., Khalil, A. A., Imran, M., Rebezov, M., … Rengasamy, K. R. R. (2020). Sesquiterpenes and their derivatives-natural anticancer compounds: An update. *Pharmacological Research, 161*, 105165.

An, Y., Quan, K. T., Gwak, J., Ju, B. G., Na, M., & Oh, S. (2018). Activation of the p53 pathway with digiferrol isolated from Rubia philippinensis induces cell cycle arrest, apoptosis, and autophagy in colon cancer cells. *Food and Chemical Toxicology, 118*, 514–522.

Chen, L. Y., Wu, Q. M., Xu, X. Y., Yang, C. H., Yang, J. B., Chen, F. L., & Zeng, Y. F. (2021). Cancer/testis antigen LDHC promotes proliferation and metastasis by activating the PI3K/Akt/GSK-3β-signaling pathway and the in lung adenocarcinoma. *Experimental Cell Research, 398*, 112414.

Choi, E. J., & Kim, C. H. (2009). Apigenin causes G2/M arrest associated with the modulation of p21Cip1and Cdc2 and activates p53-dependent apoptosis Pathway in human breast cancer SK-BR-3 cells. *Journal of Nutritional Biochemistry, 20*, 285–290.

Dehkordi, M. F., Farhadian, S., Abdolvand, M., Soureshjani, E. H., Rahmani, B., & Darzi, S. (2021). Deciphering the DNA-binding affinity, cytotoxicity and apoptosis induce as the anticancer mechanism of Bavachinin: An experimental and computational investigation. *Journal of Molecular Liquids, 341*, 117373.

Dou, X. J., Zhou, Z. Q., Ren, R. M., & Xu, M. J. (2020). Apigenin, flavonoid component isolated from Gentiana veitchiorum flower suppresses the oxidative stress through LDLR-LCAT signaling pathway. *Biomedicine & Pharmacotherapy, 128*, 110298.

Fan, X. R., Zhou, J. Y., Bi, X. W., Liang, J. J., Lu, S., Yan, X. T., … Yin, Z. M. (2021). L-theanine suppresses the metastasis of prostate cancer by downregulating MMP9 and Snail. *Journal of Nutritional Biochemistry, 89*, 108556.

Feng, H. S., Li, M. G., Altawil, A., Yin, Y., Zheng, R., & Kang, J. (2021). Cigarette smoke extracts induce apoptosis in Raw264.7 cells via endoplasmic reticulum stress and the intracellular Ca2 + / P38 /STAT1 pathway. *Toxicology in Vitro, 77*, 105249.

He, J., Ning, C. W., Wang, Y., Ma, T. F., Huang, H., Ge, Y. B., … Jiang, Y. Q. (2015). Natural plant flavonoid apigenin directly disrupts Hsp90/Cdc37 complex and inhibits pancreatic cancer cell growth and migration. *Journal of Functional Foods, 18*, 10–21.

Janssen, P. K., Mensink, R. P., Cox, F. J. J., Harryvan, J. L., Hovenier, R., Hollman, P. C. H., & Katan, M. B. (1998). Effects of the flavonoids quercetin and apigenin on hemostasis in healthy volunteers: Results from an in vitro and a dietary supplement study[1–3]. *American Journal of Clinical Nutrition, 67*, 255–262.

Jayasooriya, R. G. P. T., Dilshara, M. G., Karunarathne, W. A. H. M., Molagoda, I. M. N., Choi, Y. H., & Kim, G. Y. (2018). Camptothecin enhances c-Myc-mediated endoplasmic reticulum stress and leads to autophagy by activating Ca2+-mediated AMPK. *Food and Chemical Toxicology, 121*, 648–656.

Kaur, B., Mukhlis, Y., Natesh, J., Penta, D., & Meeran, S. M. (2022). Identification of hub genes associated with EMT-induced chemoresistance in breast cancer using integrated bioinformatics analysis. *Gene, 809*, 146016.

Ke, W. W., Zhao, X. X., & Lu, Z. M. (2021). Foeniculum vulgare seed extract induces apoptosis in lung cancer cells partly through the down-regulation of Bcl-2. *Biomedicine & Pharmacotherapy, 135*, 111213.

Kim, H. J., Kang, S., Kim, D. Y., You, S., Park, D., Oh, S. C., & Lee, D. H. (2019). Diallyl disulfide (DADS) boosts TRAIL-Mediated apoptosis in colorectal cancer cells by inhibiting Bcl-2. *Food and Chemical Toxicology, 125*, 354–360.

Kim, Y., Kim, E., & Kim, Y. (2019). l-histidine and l-carnosine accelerate wound healing via regulation of corticosterone and PI3K/Akt phosphorylation in d-galactose-induced aging models in vitro and in vivo. *Journal of Functional Foods, 58*, 227–237.

Lee, D. E., Jang, E. H., Bang, C., Kim, G. L., Yoon, S. Y., Lee, D. H., … Kim, J. H. (2021). Bakuchiol, main component of root bark of Ulmus davidiana var. japonica, inhibits TGF-β-induced in vitro EMT and in vivo metastasis. *Archives of Biochemistry and Biophysics, 709*, 108969.

Lee, H. Y., Lee, G. H., Kim, H. K., & Chae, H. J. (2019). Platycodi Radix and its active compounds ameliorate against house dustmite-induced allergic airway inflammation and ER stress and ROS by enhancing anti-oxidation. *Food and Chemical Toxicology, 123*, 412–423.

Lee, Y., Sung, B., Kang, Y. J., Kim, D. H., Jang, J. Y., Hwang, S. Y., …, Kim, N. D., (2014). Apigenin-induced apoptosis is enhanced by inhibition of autophagy formation in HCT116 human Colon cancer cells. *International Journal of Oncology 44*, 1599–1606.

Li, F., Guo, D. W., Zhi, S. F., Jia, K. Q., Wang, Y. X., Zhang, A. B., … Hao, J. (2022). Etoposide-induced protein 2.4 ameliorates high glucose-induced epithelial-mesenchymal transition by activating adenosine monophosphate-activated protein kinase pathway in renal tubular cells. *International Journal of Biochemistry and Cell Biology, 142*, 106117.

Li, X. L., Chen, M. C., Yao, Z. C., Du, H. Z., Zhang, T. F., Wang, H. Y., … Li, Z. N. (2021). Jujuboside B induces mitochondrial-dependent apoptosis in colorectal cancer through ROS-mediated PI3K/Akt pathway in vitro and in vivo. *Journal of Functional Foods, 87*, 104796.

Li, X. L., Ma, R. H., Ni, Z. J., Thakur, K., Cespedes-Acuna, C. L., Wang, S. Y., … Wei, Z. J. (2021). Dioscin inhibits human endometrial carcinoma proliferation via G0/G1 cell cycle arrest and mitochondrial-dependent signaling pathway. *Food and Chemical Toxicology, 148*, 111941.

Liu, J. Z., Liu, Y. Z., Li, H. C., Wei, C. C., Mao, A. W., Liu, W. Y., & Pan, G. F. (2022). Polyphyllin D induces apoptosis and protective autophagy in breast cancer cells through JNK1-Bcl-2 pathway. *Journal of Ethnopharmacology, 10*, 114591.

Liu, J., Peng, Y. H., & Wei, W. Y. (2021). Cell cycle on the crossroad of tumorigenesisand cancer therapy. *Trends in Biochemical Sciences, 32*, 30–44.

Liu, Z. Y., Wu, X. P., Dai, K., Li, R. K., Zhang, J. M., Sheng, D. K., … Li, J. J. (2021). The new andrographolide derivative AGS-30 induces apoptosis inhuman colon cancer cells by activating a ROS-dependent JNK signaling pathway. *Phytomedicine, 94*, 153824.

Maduni, J., Maduni, I. V., Gajski, G., Popi, J., & Vrhovac, V. G. (2018). Apigenin: A dietary flavonoid with diverse anticancer properties. *Cancer Letters, 413*, 11–22.

Morala, N. P., Sahaa, S., Philoa, M., Harta, D. J., Winterbonea, M. S., Hollandsa, W. J., … Curtisc, P. J. (2018). Comparative bio-accessibility, bioavailability and bioequivalence of quercetin, apigenin, glucoraphanin and carotenoids from freeze-dried vegetables incorporated into a baked snack versus minimally processed vegetables: Evidence from in vitro models and a human bioavailability study. *Journal of Functional Foods, 48*, 410–419.

Marina, Z., Amin, I., Loh, S. P., Fadhilah, J., & Kartinee, K. (2019). Bioaccessibility of apigenin from Mangifera indica (Water Lily Var.) during in vitro gastrointestinal digestion. *International Food Research Journal, 26*, 1627–1634.

Ma, R. H., Ni, Z. J., Zhang, F., Zhang, Y. Y., Liu, M. M., Thakur, K., … Wei, Z. J. (2020). 6-Shogaol mediated ROS production and apoptosis via endoplasmic reticulum and mitochondrial pathways in human endometrial carcinoma Ishikawa cells. *Journal of Functional Foods, 74*, 104178.

Ma, W. D., Zou, Y. P., Wang, P., Yao, X. H., Sun, Y., Duan, M. H., … Yu, B. (2014). Chimaphilin induces apoptosis in human breast cancer MCF-7 cells through a ROS-mediated mitochondrial pathway. *Food and Chemical Toxicology, 70*, 1–8.

Madunic, J., Maduni, I. V., Gajski, G., Popi, J., & Garaj-Vrhovac, V. (2018). Apigenin: A dietary flavonoid with diverse anticancer properties. *Cancer Letters., 413*, 11–22.

Manogaran, P., Beeraka, N. M., Huang, C. Y., & Padma, V. V. (2019). Neferine and isoliensinine enhance 'intracellular uptake of cisplatin' and induce 'ROS-mediated apoptosis' in colorectal cancer cells-A comparative study. *Food and Chemical Toxicology, 132*, 110652.

Marunaka, Y., Niisato, N., Zou, X. B., Xiao, J. B., & Nakahari, T. (2020). Food intake targeting and improving acidity in diabetes and cancer. *Food Frontiers, 1*, 9–12.

Nielsen, S. E., Young, J. F., Daneshvar, B., Lauridsen, S. T., Knuthsen, P., Sandström2, B., & Dragsted, L. O., (1999). Effect of parsley (Petroselinum crispum) intake on urinary apigenin excretion, blood antioxidant enzymes and biomarkers for oxidative stress in human subjects. *British Journal of Nutrition. 81,* 447–455.

Omar, H., Obaya, E., Sabry, D., Abdelkader, A., Maher, M., & Mekawy, D. (2020). Apigenin inhibits proliferation of hepatocellular carcinoma cell by upregulation of cleaved caspases-3/8 and downregulation of pSTAT-3/ pJAK-1/pJAK-2. *Gene Reports, 21*, 100964.

Perera, J., & Hoskin, P. (2021). Adjuvant therapy for high-risk endometrial carcinoma. *Clinical Oncology., 33*, 560–566.

Prabhakar, P. V., Chen, Y. H., He, A. Y., Bridgitte, E. P., Ilanna, L., Liu, J. H., … Gangadhara, R. S. (2022). KDM1A inhibition augments the efficacy of rapamycin for the treatment of endometrial cancer. *Cancer Letters, 524*, 219–231.

Qin, Y., Zhang, H., Liu, Q., Jiang, B., Chen, J., & Zhang, T. (2021). Sulforaphane attenuates oxidative stress and inflammation induced by fine particulate matter in human bronchial epithelial cells. *Journal of Functional Foods, 81*, 104460.

Shrestha, S., & Clark, A. C. (2021). Evolution of the folding landscape of effector caspases. *Journal of Biological Chemistry., 297*, 101249.

Sim, H. J., Song, M. S., & Lee, S. Y. (2021). Kv3 channels contribute to cancer cell migration via vimentin regulation. *Biochemical and Biophysical Research Communications., 551*, 140–147.

Soto-Gamez, A., Wang, Y. Z., Zhou, X. Y., Seras, L., Quax, W., & Demaria, M. (2022). Enhanced extrinsic apoptosis of therapy-induced senescent cancer cells using a death receptor 5 (DR5) selective agonist. *Cancer Letters, 525*, 67–75.

Stoner, G. D. (2020). Food-based approach to cancer prevention. *Food Frontiers, 1*, 6–8.

Saripalli, A. L., Griffin, A. C., Ross, D., Roeske, J. C., Jr, W. S., & Harkenrider, M. M., (2022). Updates in adjuvant therapy for high-risk and locally advanced endometrial cancer. Advances in Oncology 2, 25–33.

Vijaya, K., Sowmyaa, P. R., Arathia, B. P., Shilpaa, S., Shwethaa, H. J., Raju, M., … Laskshiminarayana, R. (2018). Low-dose doxorubicin with carotenoids selectively alters redox status and upregulates oxidative stress-mediated apoptosis in breast cancer cells. *Food and Chemical Toxicology., 118*, 675–690.

Wang, X. R., Chen, Q., Ou, J., Huang, Y. L., Wang, C. C., Chen, Y. A., … Meng, X. M. (2022). Real-time and accurate monitoring of mitochondria-related apoptosis by a multifunctional two-photon fluorescent probe. *Sensors and Actuators: B. Chemical., 351*, 130953.

Won, Y. S., & Seo, K. I. (2020). Sanggenol L promotes apoptotic cell death in melanoma skin cancer cells through activation of caspase cascades and apoptosis-inducing factor. *Food and Chemical Toxicology, 138*, 111221.

Wu, C. H., Yang, M. Y., & Wang, C. J. (2019). Quercetin-3-O-glucuronide inhibits doxorubicin resistance by reducing endoplasmic reticulum stress in hepatocellular carcinoma cells. *Journal of Functional Foods, 54*, 301–309.

Wu, H. B., Guo, H. R., Liu, H., Cui, H. M., Fang, J., Zuo, Z. C., … Zhao, L. (2020). Copper sulfate-induced endoplasmic reticulum stress promotes hepatic apoptosis by activating CHOP, JNK and caspase-12 signaling pathways. *Ecotoxicology and Environmental Safety., 191*, 110236.

Xu, Y. N., Deng, M. S., Liu, Y. F., Yao, J., & Xiao, Z. Y. (2021). Tight junction protein CLDN17 serves as a tumor suppressor to reduce the invasion and migration of oral cancer cells by inhibiting epithelial-mesenchymal transition. *Archives of Oral Biology., 133*, 105301.

Yang, C. W., Song, J., Hwang, S., Choi, J., Song, G., & Lim, W. (2021). Apigenin enhances apoptosis induction by 5-fluorouracil through regulation of thymidylate synthase in colorectal cancer Cells. *Redox Biology, 47*, 102144.

Yang, C. W., Song, J., Hwang, S., Choi, J., Song, G., & Lim, W. (2021). Apigenin enhances apoptosis induction by 5-fluorouracil through regulation of thymidylate synthase in colorectal cancer cells. *Redox Biology, 47*, 1021144.

Yang, J. L., Pi, C. C., & Wang, G. H. (2018). Inhibition of PI3K/Akt/mTOR pathway by apigenin induces apoptosis and autophagy in hepatocellular carcinoma cells. *Biomedicine & Pharmacotherapy, 103*, 699–707.

Yin, Q., Chen, H., Ma, R. H., Zhang, Y. Y., Liu, M. M., Thakur, K., … Wei, Z. J. (2021). Ginsenoside CK induces apoptosis of human cervical cancer HeLa cells by regulating autophagy and endoplasmic reticulum stress. *Food & Function, 12*, 5301–5316.

Yu, S., Jia, B. X., Yang, Y. X., Liu, N., & Wu, A. B. (2020). Involvement of PERK-CHOP pathway in fumonisin B1-induced cytotoxicity in human gastric epithelial cells. *Food and Chemical Toxicology, 136*, 111080.

Zhang, F., Zhang, Y. Y., Sun, Y. S., Ma, R. H., Thakur, K., Zhang, J. G., & Wei, Z. J. (2020). Asparanin a from asparagus officinalis L. Induces G0/G1 cell cycle arrest and apoptosis in human endometrial carcinoma Ishikawa cells via mitochondrial and PI3K/AKT signaling pathway. *Journal of Agricultural and Food Chemistry, 68*, 213–224.

Zhang, J. X., Liang, Y., Lin, Y. B., Liu, Y. B., You, Y., & Yin, W. Q. (2016). IRE1α-TRAF2-ASK1 pathway is involved in CSTMP-induced apoptosis and ER stress in human non-small cell lung cancer A549 cells. *Biomedicine & Pharmacotherapy, 82*, 281–289.

Zhang, W. J., Luo, C., Huang, C., Pu, F. Q., Zhu, J. F., & Zhu, Z. M. (2021). PI3K/Akt/GSK-3β signal pathway is involved in P2X7 receptor-induced proliferation and EMT of colorectal cancer cells. *European Journal of Pharmacology, 899*, 174041.

Zhang, X. S., Kan, H., Liu, Y., & Ding, W. (2021). Plumbagin induces Ishikawa cell cycle arrest, autophagy, and apoptosis via the PI3K/Akt signaling pathway in endometrial cancer. *Food and Chemical Toxicology, 148*, 111957.

Zou, X. J., Liang, J. Y., Sun, J. Y., Hu, X. Y., Lei, L., Wu, D. H., & Liu, L. (2016). Allicin sensitizes hepatocellular cancer cells to anti-tumor activity of 5-fluorouracil through ROS-mediated mitochondrial pathway. *Journal of Pharmacological Sciences, 131*, 233–240.